

# The stochastic gravitational-wave background exists permanently and has time-domain asymmetry

Alexander V. Kramarenko<sup>a,\*</sup>, Andrey V. Kramarenko<sup>b</sup>, Oksana O. Savenko<sup>c</sup>

<sup>a</sup>TREDEX Company Ltd., PO box 11515, Kharkiv, Ukraine 61001

<sup>b</sup>General and Inorganic Chemistry Department, National Technical University “KhPI”, 2 Kyrpychova str., Kharkiv, Ukraine 61002

<sup>c</sup>School of Physics and Technology, V. N. Karazin Kharkiv National University, 4 Svobody Sq., Kharkiv, Ukraine 61022

## Abstract

Analyzing the records of Advanced LIGO and Virgo gravitational observatories, we found a specific time-domain asymmetry, inherent only to the signals of their gravitational detectors. Experiments with different periodic signals, Gaussian and non-Gaussian noises made it possible to conclude that the noise of gravitational detectors is an unusual mixture of signals. The gravitational-wave signals have been detected and recognized using a specialized Pearson correlation analyzer. It turned out that the detector signals include a significant (−6 dB) component, which has the properties of records of reliably recognized gravitational waves. This allows one to argue that the gravitational noise is largely due to the processes of merging astronomical objects. Since the specific signal is registered by the detectors continuously, the field of gravitational oscillations of the sub-kilohertz band can be considered as detected. A method of analysis has also been developed to estimate the contribution of the gravitational noise component to the total signal energy. With its help it will be possible not only to pass to the radio-frequency estimation of the magnitude of gravitational disturbances but also, possibly, to construct a map of the gravitational noise of the sky.

## 1 Introduction

By now, the gravitational-wave events detected by the Advanced LIGO<sup>1</sup> and Virgo<sup>2</sup> observatories are the pulse signals having combined frequency and amplitude modulation, smooth rise and sharp roll-off<sup>3</sup>. The linear frequency modulated (LFM) or “chirp” radar signals<sup>4</sup> have a similar time-domain asymmetry in frequency only while the pulse amplitude does not change significantly.

The optimal detector of a signal with such a specific form would be convolution with its time-inverted copy<sup>5</sup> because the convolution with the noninverted copy gives a much smaller response not concentrated in time. This is caused by the time-domain asymmetry of pulses.

As far as we know, the question about the contribution of gravitational waves due to the merging of rotating masses to the stochastic background gravitational-wave noise is currently topical, widely discussed in a number of articles<sup>6,7,8,9,10,11</sup>, and far from being finally solved. We should separately mention the article<sup>7</sup>, the authors of which proposed a method of detecting stellar mass merger events based on small differences between the observed noise and the Gaussian noise.

---

\* Principal corresponding author

Email addresses: tredexcompany37@gmail.com (Alexander V. Kramarenko), andrii.kramarenko@kphi.edu.ua (Andrey Kramarenko), xana.savenko@gmail.com (Oksana O. Savenko)

But the Gaussian criteria in no way forbid noise to be symmetric or asymmetric in time.

Let us take a sufficiently large realization of ideal white Gaussian noise and divide it into a set of equal fragments. After spectral analysis, we calculate the median frequency of the spectrum of each fragment. Let us assemble a new realization from the fragments, where the first fragments will have low median frequencies of the spectrum, the second will have middle median frequencies, the third will have high median frequencies, and so on cyclically. The resulting realization will fully correspond to all the criteria of the Gaussian white noise (GWN), as the original one. Neither the distribution function nor spectrum of the new realization does not differ from the original ones. But the spectrum analyzer with a sliding window equal to the length of the fragment, when shifting from left to right along the new realization, generates no longer a random but the cyclic sequence of median frequencies. Being played again in a backward direction, this realization, of course, shows the same not random sequence but in the reverse order. It has gained the detectable time-domain asymmetry.

That is why the search for the asymmetry of the gravitational noise seems to us more promising than the analysis of the distribution function and spectra, because the signals of stellar mass mergers are asymmetric in the time domain.

## 2 Signal processing method

According to our method, in order to estimate the gravitational wave contribution to the total detectors' noise power, it is necessary to check: is there something in the background noise, which looks like the time-domain asymmetry of a typical gravitational wave signal? This problem must be solved only in the time domain in order to provide a linear phase response for the whole filtering system, so, preliminary spectral whitening will have to be excluded.

We have developed our own system of filtering gravitational signals, which uses only linear time-invariant elements excluding high order IIR filters<sup>12</sup>, giving exponentially decaying "tails" distorting the results. All processing is performed in the time domain exclusively. The nonrecursive FIR filter appropriate to solve the described problem is as follows:

$$W_i = -\cos \frac{2\pi i}{N-1} \cdot \sin^2 \frac{\pi i}{N-1} \quad (1)$$

where  $i \in [0, N-1]$  is the number of the count inside the window of length  $N$  counts.

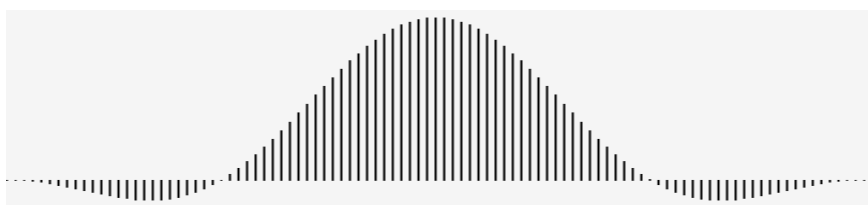


Fig. 1. FIR filter weighting window

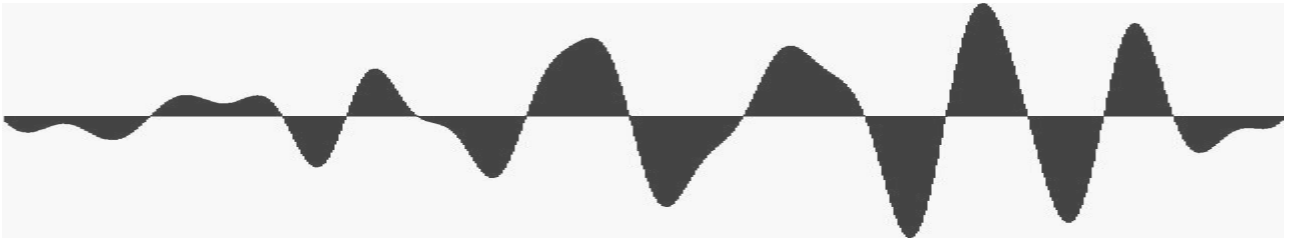


Fig. 2. Gravitational wave extracted from the original signal using our filter system. The original file [H-H1\\_GWOSC\\_16KHZ\\_R1-1185389792-32.wav](#) from the original LIGO data<sup>13</sup> contains the event GW170729<sup>14</sup>. File after filtering: [H1\\_filt.wav](#) (listening to both records is possible).

Figure 2 shows the gravitational-wave signal extracted in this way. It is frequency-limited from above, but has a minimum of out-of-band interference.

Note that the original LIGO material<sup>13</sup> (file [H-H1\\_GWOSC\\_16KHZ\\_R1-1185389792-32.wav](#)) has the signal spectrum shown in Figure 3. Of course, at such a signal-to-noise ratio it is necessary to suppress both dominant low-frequency components and high-frequency harmonics. The inevitable non-uniformity of the frequency response in the required bandwidth will be less unfavorable for the subsequent analysis than the residual out-of-band components.

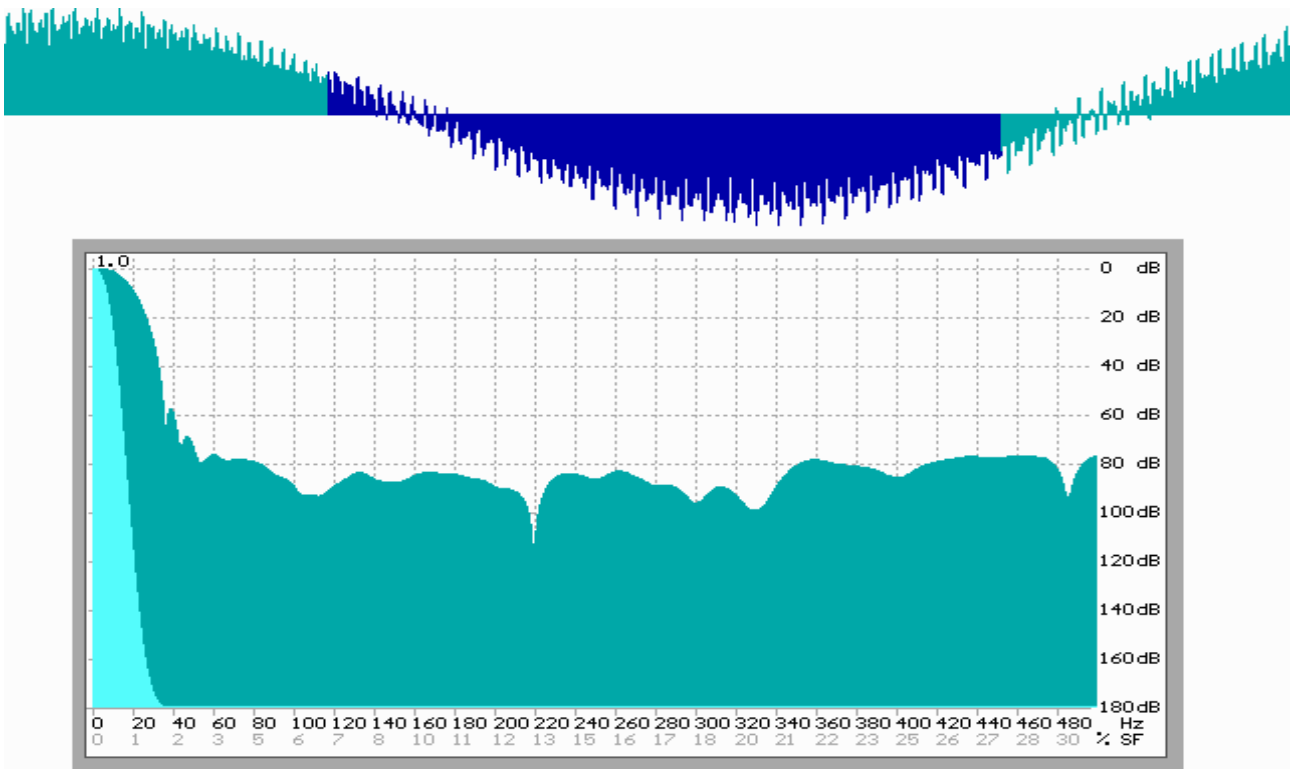


Fig. 3. Spectral estimation of the LIGO signal. The oscillogram is at the top, the area in which the gravitational wave of the event GW170729 was recorded is highlighted in blue. The energy spectrum is at the bottom, the X-axis scale is linear; the resolution is 0.5 Hz. Hann weighting window is applied, green color is the spectrum in logarithmic scale by the ordinate, light blue color shows it in linear one.

When filtering this signal the following results were obtained (see Figure 4):  $-200$  dB ( $80 + 120$ ) in the  $0 \dots 20$  Hz band and at least  $-126$  dB at frequencies above 470 Hz, which agrees well with the maximum possible suppression taking into account the residual digitization resolution.

The non-uniformity of the filter frequency response in the range of 70...250 Hz (i.e. in the least noisy range) did not exceed 6 dB.

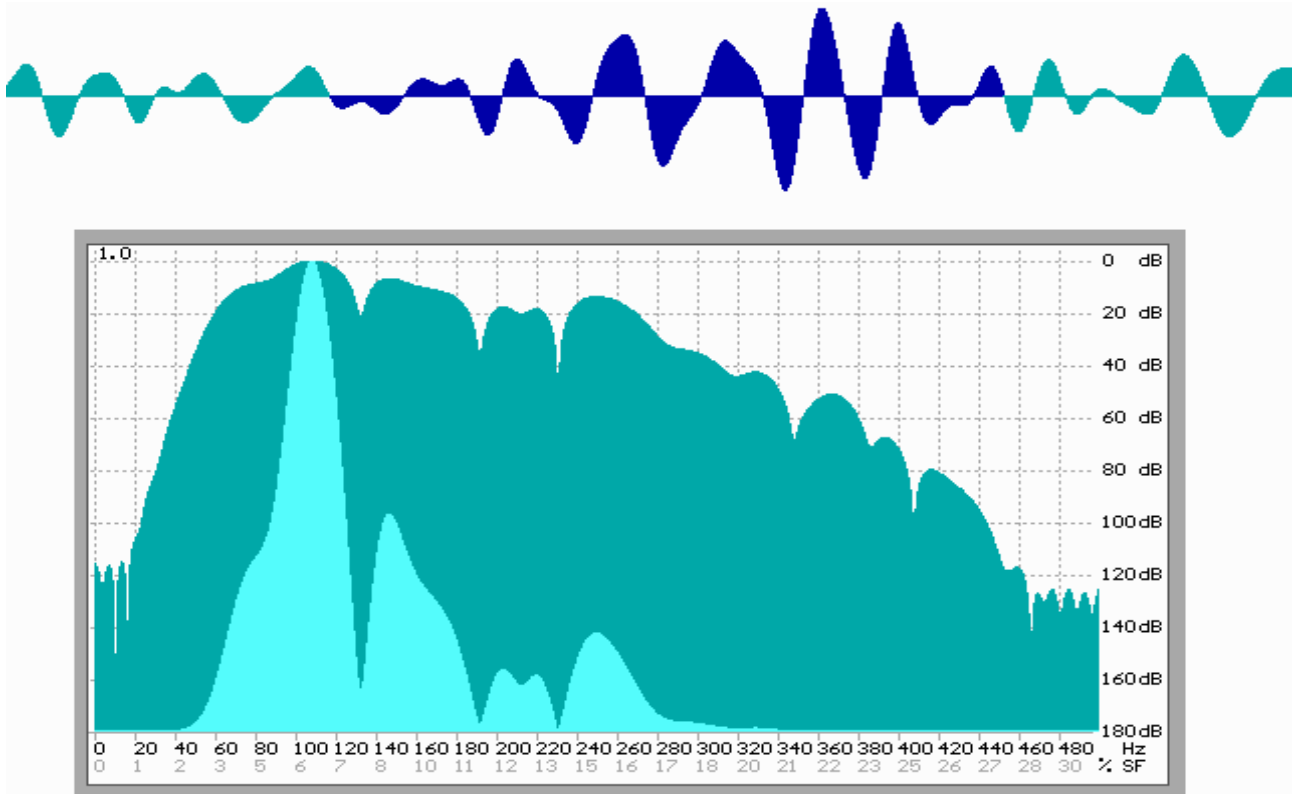


Fig. 4. Spectral estimation of the LIGO signal after FIR filtering: the signal is confidently separated from the noise, the suppression of out-of-band components is sufficient.

We can check the efficiency of the gravitational wave extraction and the correctness of the chosen filtering method by evaluating the operation of the convolutional detector. In our case we used the time-inverted gravitational wave signal by the event GW170729<sup>14</sup> as a prototype.

For each shift per count of the signal of the original file [H1\\_filt.wav](#) two parameters has been calculated: a) the square of the Pearson correlation coefficient<sup>15</sup> and b) the current fragment of the convolved signal weighted with the cosine window<sup>16</sup>  $\omega_i$ . The product of these parameters is presented as a graph unfolding synchronously with the original signal (see Figure 5):

$$V_j = \sum_{i=0}^{N-1} X_i \left[ \frac{\left(1 - \cos \frac{2\pi i}{N-1}\right) \times \left(\sum_{k=0}^{N-1} (X_k - \bar{X})(Y_k - \bar{Y})\right)^2}{\sum_{k=0}^{N-1} (X_k - \bar{X})^2 \sum_{k=0}^{N-1} (Y_k - \bar{Y})^2} \right]^2 = \sum_{i=0}^{N-1} \frac{X_i \omega_i [\text{cov}(X, Y)]^2}{s^2(X) \cdot s^2(Y)}; \quad (2)$$

where  $V_j$  is the count of the output signal,  $X$  is the realization of the input signal,  $Y$  is the realization of the inverse prototype,  $n$  is the length of realizations (in number of counts),  $s^2$  is the variance of samples. The values of  $V_j$  are always positive and will be the greater as realization of  $X$  correlates stronger with the prototype of  $Y$  and the signal level of  $X$  is higher.

To confirm the hypothesis about time-domain asymmetry of gravitational noise over time, it

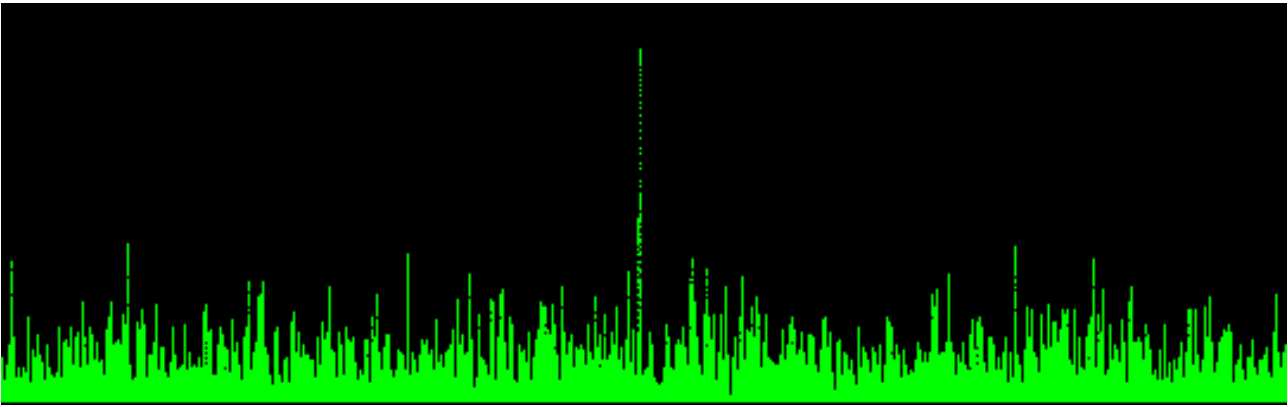


Fig. 5. Time series of  $V_j$  values calculated by formula (2) for file [H1\\_filt.wav](#). The duration of the recording fragment is 24 seconds. In the middle of the graph there is a response from the "officially confirmed" wave, at least three more bursts correspond to the fragments, about which there was a discussion about the correspondence of their form to the gravitational wave pattern.

should be experimentally recorded and, if possible, measured. Detection and recognition of gravitational wave signals were carried out using a specialized Pearson<sup>15</sup> correlation analyzer.

Our basic idea is that (for a sufficiently long realization) the statistically accumulated Pearson correlations of any time-symmetric signal (noise) with the direct and inverted prototypes will always be equal.

Here, apparently, it is necessary to explain the idea by means of a simple model. So, let's introduce a long digitized realization of Gaussian noise, and a short fragment of signal having time-domain asymmetry: for example, a digitized sound of Euler's falling disk<sup>17</sup> or an chirp (LFM) radar pulse. Now let this signal fragment slide along the realization of the noise. Calculating the Pearson coefficient at each step, we can make sure that at any time the value of process correlation will fluctuate between  $-1.0 < R < +1.0$ . The accumulated sum of all coefficients will tend to zero, since the noise is not correlated with the signal.

If you reverse any of the signals in time, i.e. "backwards", and repeat the measurement, the result will be identical: the sum of the accumulated coefficients will tend to zero, and this is expected, since the noise is symmetrical in the time domain – it can be viewed from left to right or vice versa – nothing will change.

A completely different result will be obtained if the noise itself (NB!) consists of fragments of asymmetric in time signals. Suppose we have collected sounds of a very large number of simultaneously rotating and falling Euler disks. According to the central limit theorem, the total signal will be band-limited noise. Its statistical characteristics will be close to Gaussian (the closer, the more discs launched simultaneously). When calculating the correlation of this noise with a fragment of its generating signal, the following phenomenon must appear: the accumulated sum of correlations will depend on the direction of mutual displacement of the signals. And if at least one of signals is symmetric in time, there will be no asymmetry at accumulation of correlations, and the

phenomenon will appear only if both (NB!) signals are asymmetric.

Let us perform processing of the real signals. To exclude the influence of signal amplitude on the result we will use only normalized correlation with the direct and inverse prototype. We will accumulate the difference of correlation coefficients for each sample of the signal and present it as a graph synchronous with the work of the detector, i.e.:

$$R_j = R_{j-1} + \left[ \frac{\sum_{k=0}^{N-1} (X_k - \bar{X})(Y_k - \bar{Y})}{\sqrt{\sum_{k=0}^{N-1} (X_k - \bar{X})^2 \sum_{k=0}^{N-1} (Y_k - \bar{Y})^2}} - \frac{\sum_{k=0}^{N-1} (X_k - \bar{X})(Z_k - \bar{Z})}{\sqrt{\sum_{k=0}^{N-1} (X_k - \bar{X})^2 \sum_{k=0}^{N-1} (Z_k - \bar{Z})^2}} \right] =$$

$$= R_{j-1} + \frac{\text{cov}(X, Y)}{\sigma(X)\sigma(Y)} - \frac{\text{cov}(X, Z)}{\sigma(X)\sigma(Z)};$$
(3)

where  $X$  is the input signal array,  $Y$  is the inverse prototype, and  $Z$  is the non-inverse prototype.

Obviously, if the signals are statistically symmetric over time, the curve of time dependence  $R$  will not deviate significantly either in the positive or in the negative region, i.e. accumulation will not occur. If the signal is asymmetric, the curve will shift monotonically up or down.

### 3 Results and discussion.

As a zero reference, we first investigate the white normally distributed Gaussian noise that passes through our filtering system (file [N\\_filt.wav](#)). At the beginning and at the end of the implementation, replace the noise with a monochromatic signal for clarity and convenience in evaluating the results (see Figure 6).

Note that during the observation time (30 s) there is no accumulated asymmetry, despite periodic small deviations in both directions. The same results were observed for all other noise, unmodulated harmonic signals, and any noise/signal combinations.

In the search for asymmetric processes, musical works were also used, as the variety of instruments and melodies, modulation by frequency, amplitude and timbre, it would seem, should manifest itself in the asymmetry on the time scale. The most significant fluctuations in the  $R$  graph are obtained in recordings of a symphony orchestra with chorus, but the accumulation of asymmetry does not occur (see Figure 7).

Completely different effects were observed in the analysis of real gravitational signals. For the Hanford Observatory, the shift of the correlation plot is confidently fixed. If we increase the observation time, the asymmetry will continue to grow monotonically (see Figure 8).

The vicinity of the most powerful gravitational wave is interesting with some anomaly lasting for units of seconds (the duration of the recording fragment is 30 seconds: the beginning and the end of the fragment are replaced by a monochromatic signal).

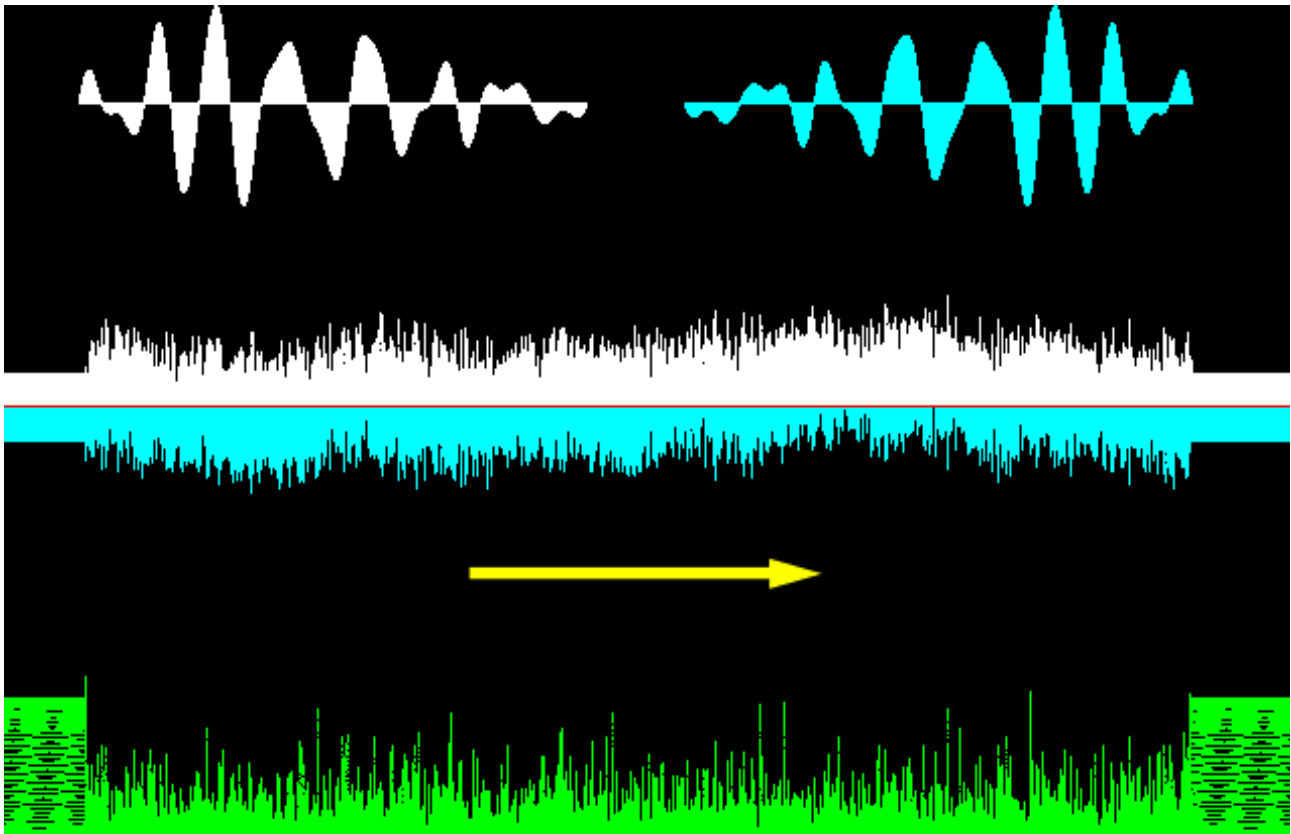


Fig. 6. Estimation of the asymmetry of the noise signal. At the top the prototypes with which the signal is convolved: light gray shows the time-inverted "direct" pattern  $Y$ , blue indicates the noninverted "inverse" pattern  $Z$ . In the middle is shown the graph of accumulation of difference  $R_j$  of Pearson coefficients, i.e. the value of asymmetry. At the bottom, the time series  $V_j$  is shown. The yellow arrow shows the direction of the time axis.

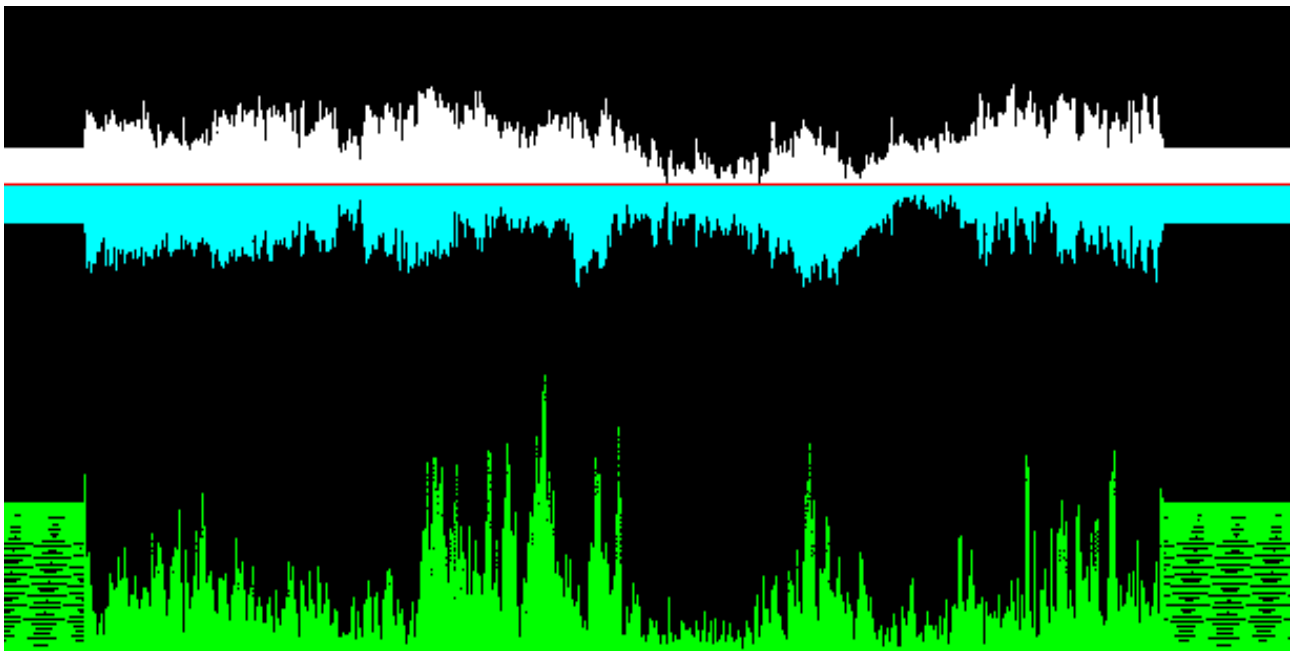


Fig. 7. Music signal analysis. Source file: [music.wav](#); filtered file: [mus\\_filt.wav](#). Despite the fluctuations of the graph, the accumulated asymmetry is equal to zero.

For the records from the Livingstone Observatory, the asymmetry is even larger (see Figure 9). Unfortunately, detector (2) does not record any obvious bursts, which is probably due

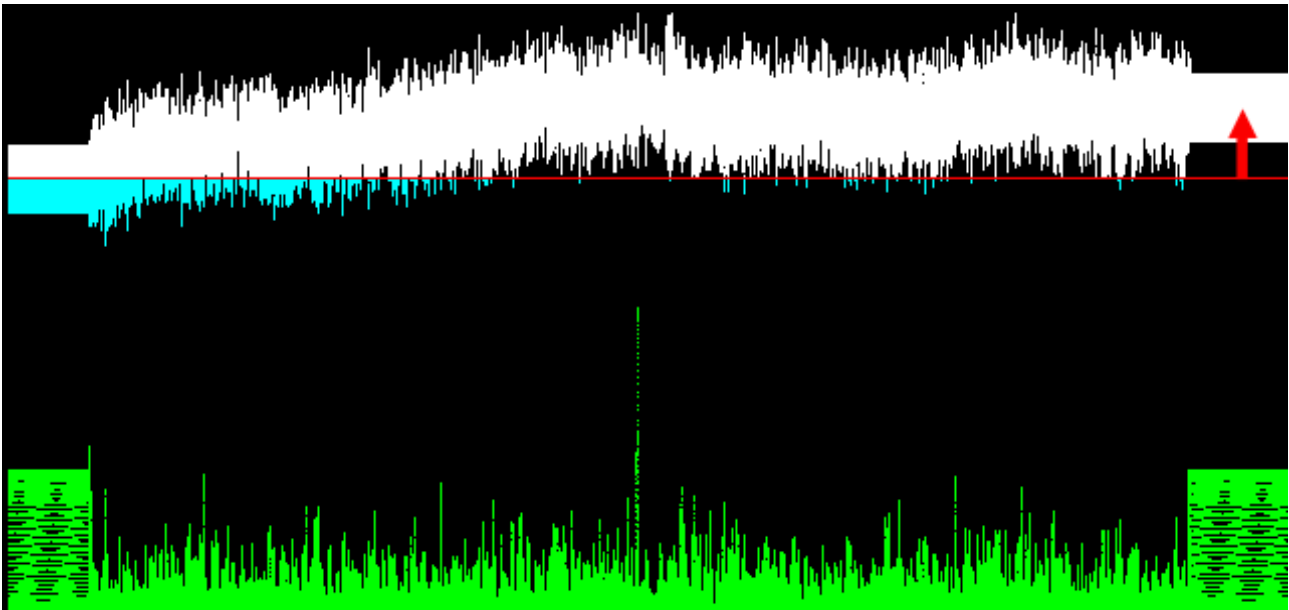


Figure 8. Hanford Observatory. Processing of the file [H1\\_filt.wav](#) (original [H1\\_GWOSC\\_16KHZ\\_R1-1185389792-32.wav](#)). In contrast to the noise signals, the accumulated asymmetry is not equal to zero. The red arrow shows the rise of the plot.

to the prototype, which is isolated from the Hanford recordings-the signal shapes are apparently somewhat different.

The worst, but, nevertheless, comparable results are obtained for the Virgo records (Figure 10). Unfortunately, the frequency drifting fan noise cannot be filtered out completely (the data of the compensation channels provided by the LIGO observatory<sup>18</sup> were not used in our work, since, unfortunately, they are not available for the event GW170729).

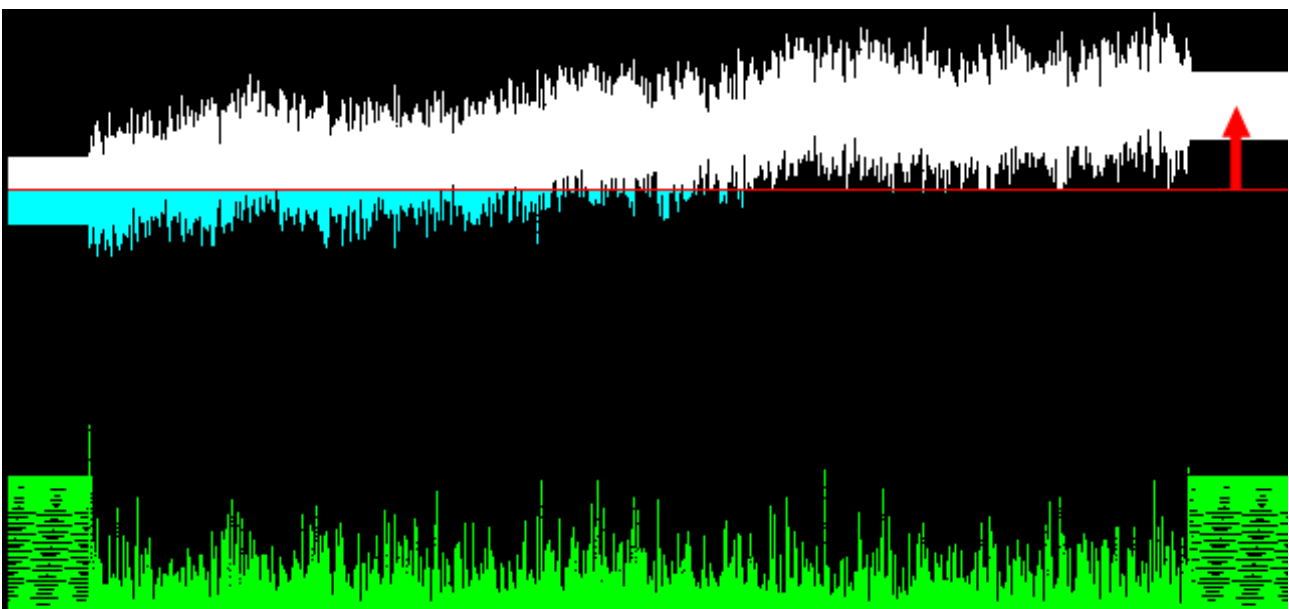


Fig. 9. Livingston Observatory. Processing of file [L1\\_filt.wav](#) (original file [L-L1\\_GWOSC\\_16KHZ\\_R1-1185389792-32.wav](#)). The asymmetry is clearly observed.

It should be noted that for the LIGO recordings, the accumulated asymmetry is unequal: all signal registrations after hardware upgrades, i.e., reduction of intrinsic noise and improvement of

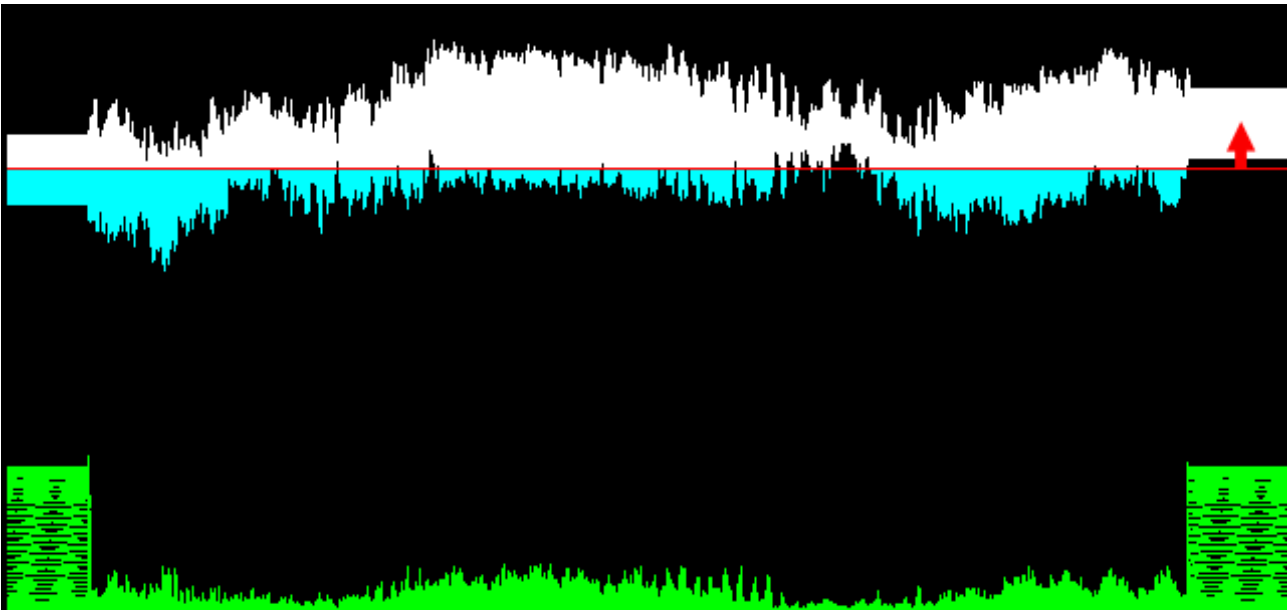


Fig. 10. Virgo Observatory. File [V1\\_filt.wav](#) (original [V-V1\\_GWOSC\\_16KHZ\\_R1-1185389792-32.wav](#)). Due to unsuppressed hardware interference, the detector does not work well. The signal asymmetry is unquestionable, but it is lower than in the previous illustrations.

the signal-to-noise ratio, give a more asymmetric signal (which is to be expected).

So, in all records of gravitational noise one observes asymmetry in time, i.e. the contribution of gravitational wave components is stably detected. Comparing these records with various periodic signals, Gaussian and non-Gaussian noises made it possible to draw a preliminary conclusion that the noise of gravitational detectors is a unique kind of signal. But this is only a qualitative estimate. For quantitative estimates it is necessary to find some non-trivial method of measurement.

It is impossible in principle to separate hardware, seismic, thermal, Newtonian noise from gravitational noise. A basic statement of information theory states: “If signals exist simultaneously, and their spectra overlap, then complete separation of signals is impossible.”

In our case, the only way to solve the problem remains: modeling signals with a known additive contribution of gravitational wave components to the structure of the Gaussian noise.

Let us make a measurement with a known high contribution of the “gravitational” component: let us add to the Gaussian noise fragments of the officially registered gravitational wave so that the signal to noise ratio is 3:1, (Figure 11, at such a ratio the signal against the noise will already be observed visually).

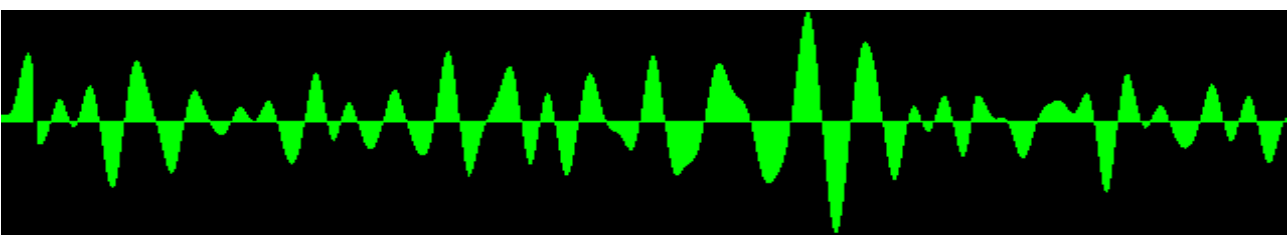


Fig. 11. Additive mixture of the components of gravitational waves and GWN in the ratio 3:1. As expected, the characteristic patterns are visually detectable.

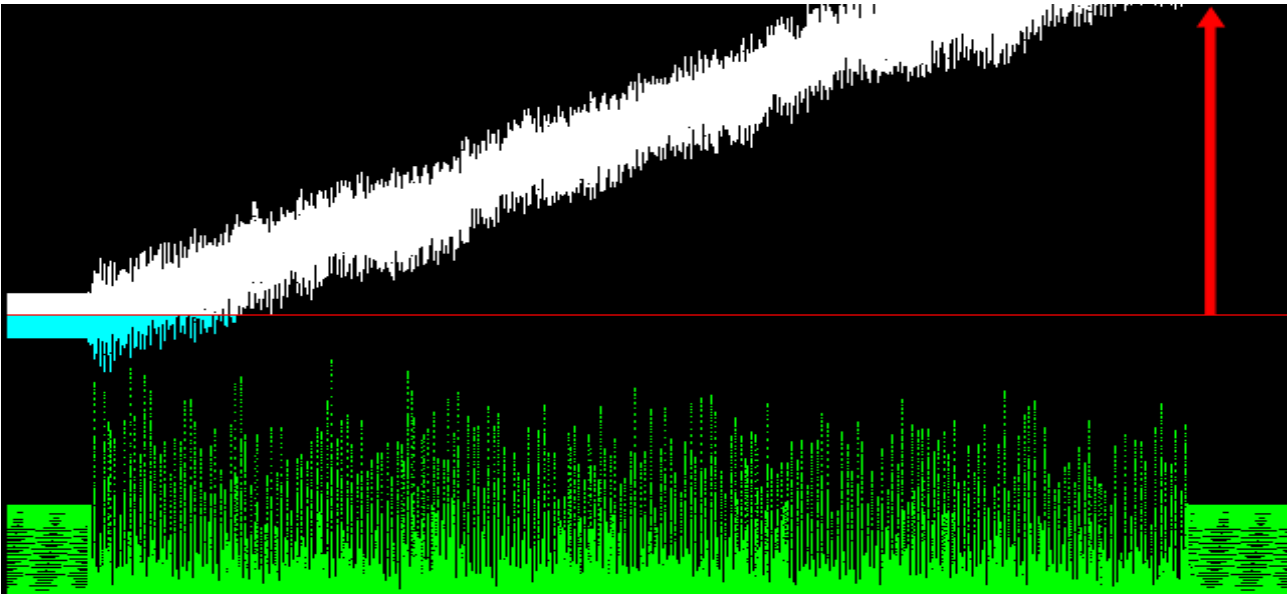


Fig. 12. Analyzer performance with a significant contribution of the "gravitational" component. The signal-to-noise ratio is 3:1. Multiple  $V_j$  spikes are detected. The asymmetry is large, the accumulated difference of Pearson coefficients grows rapidly.

Let us estimate the accumulation of asymmetry and monitor the detector performance (Figures 12 and 13). We will assume that the measuring instrument is pre-tested, and it is possible to select such a signal-to-noise ratio, which will allow to reach the values of the curve rise as in the cases of gravitational detector signal recordings.

Here we can add that partial separation of noise components is possible in the time domain, i.e. the signal is divided into two channels in a correlation way: asymmetric (left channel) and symmetric (right channel) noises (Figure 14). The [stereo2.wav](#) file, when listened to, gives an idea of how the purely noise and "gravitational" components differ (powerful pulses in the left channel at the 15th second correspond to the event GW170729).

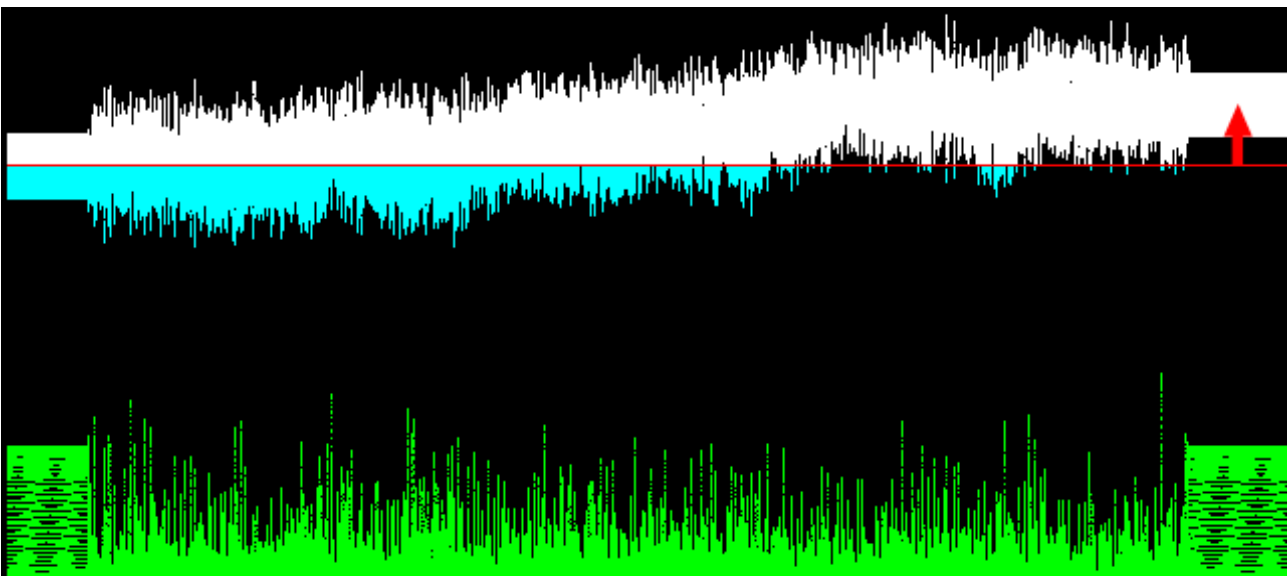


Fig. 13. The signal-to-noise ratio is 1:2. Complete correspondence to the average value of the asymmetry for the records of gravitational detectors. The estimate is, of course, preliminary.

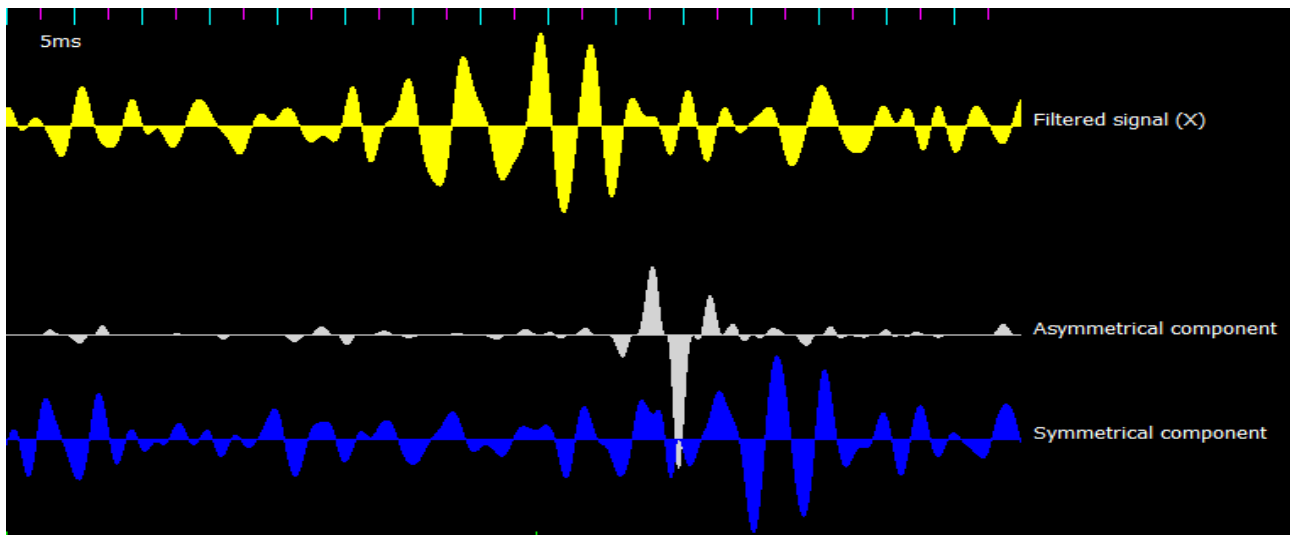


Fig. 14. The signal of event GW170729 after the filter (1) and its asymmetric and symmetric (in time) components. The time delay in the appearance of symmetric signals can be clearly seen. The reason for this phenomenon is not yet clear to the authors, but we can assume that the appearance of delayed signals due to the interaction of the gravitational wave with the mass of the Earth.

We also are pleased to present the working version of the analyzer program that we developed, with the help of which we obtained the results published here. A program (together with the brief instruction on how to use) is inside the [archive file](#). The file size is 23M.

### 3. Conclusions

The results of indirect measurements allow us to conclude that the continuous gravitational noise at the output of the detectors is approximately  $-6$  dB, and this, in fact, is an unexpectedly<sup>10</sup> large value. So, the rarely observed high-amplitude gravitational waves and the essential part of continuous noise due to the same process, namely the merging of massive astronomical objects.

The very presence of asymmetry of the signal received by detectors means that there is a stochastic gravitational-noise field of sub-kilohertz band so any optical and radio-frequency signals always propagate in it. Then the input signal of any visual or radio telescope directed to any point of space will include a ripple caused by gravitational noise<sup>19,20</sup> and manifested as a differential modulation in the azimuth and angle of location in the picture plane of the observer (i.e. the change in the scattering ellipse and/or polarization). Accordingly, at the output of the quadrature polarimeter with measurement time less than 1 ms and bandwidth limitation at frequencies below 70 Hz there will be an additive mixture of intrinsic noise and gravitational noise component, which can now be estimated (although it is still impossible to completely separate these noises).

The contribution of gravitational background may be small, but with increasing of realization, i.e. registration time, the accuracy of measurement will increase. Then maps of the gravitational noise of the sky can be obtained with the available radio telescopes. In addition, the relic radiation should also have traces of propagation in the gravitational noise field.

## References

1. Aasi, J. *et al.* Advanced LIGO. *Class. Quantum Gravity* **32**, (2015).
2. Acernese, F. *et al.* Advanced Virgo: a second-generation interferometric gravitational wave detector. *Class. Quantum Gravity* **32**, 024001 (2014).
3. Sturani, R. *et al.* Complete phenomenological gravitational waveforms from spinning coalescing binaries. *J. Phys. Conf. Ser.* **243**, 012007 (2010).
4. Klauder, J. R., Price, A. C., Darlington, S. & Albersheim, W. J. The theory and design of chirp radars. *Bell Syst. Tech. J.* **39**, 745–808 (1960).
5. Nikolaev, A. P., Krivonozhko, I. . S. & Sobkina, N. Y. Target travel compensation on long-term accumulation of radar signals. *Journal of «Almaz – Antey» Air and Space Defence Corporation* 12–19 (2018).
6. Littenberg, T. B. & Cornish, N. J. Bayesian inference for spectral estimation of gravitational wave detector noise. *Phys Rev D* **91**, 084034 (2015).
7. Smith, R. & Thrane, E. Optimal Search for an Astrophysical Gravitational-Wave Background. *Phys Rev X* **8**, 021019 (2018).
8. Allen, B. & Romano, J. D. Detecting a stochastic background of gravitational radiation: Signal processing strategies and sensitivities. *Phys Rev D* **59**, 102001 (1999).
9. Regimbau, T. The astrophysical gravitational wave stochastic background. *Res. Astron. Astrophys.* **11**, 369–390 (2011).
10. Abbott, B. P. *et al.* GW150914: Implications for the Stochastic Gravitational-Wave Background from Binary Black Holes. *Phys Rev Lett* **116**, 131102 (2016).
11. George, D. & Huerta, E. A. Deep Learning for real-time gravitational wave detection and parameter estimation: Results with Advanced LIGO data. *Phys. Lett. B* **778**, 64–70 (2018).
12. Lai, E. 7 - Infinite impulse response (IIR) filter design. in *Practical Digital Signal Processing* (ed. Lai, E.) 145–170 (Newnes, 2003). doi:10.1016/B978-075065798-3/50007-2.
13. GW170729. *Gravitational Wave Open Science Center*  
<https://www.gw-openscience.org/eventapi/html/GWTC-1-confident/GW170729/v1/>.
14. Abbott, B. P. *et al.* GWTC-1: A Gravitational-Wave Transient Catalog of Compact Binary Mergers Observed by LIGO and Virgo during the First and Second Observing Runs. *Phys Rev X* **9**, 031040 (2019).

15. Stationary Random Processes. in *Random Data* 109–171 (John Wiley & Sons, Ltd, 2010).  
doi:<https://doi.org/10.1002/9781118032428.ch5>.
16. Barros, J. & Diego, R. I. On the use of the Hanning window for harmonic analysis in the standard framework. *IEEE Trans. Power Deliv.* **21**, 538–539 (2006).
17. Abbott, P., Keady, G. & Tyler, S. Euler’s disk: examples used in engineering and applied mathematics teaching. in *Proceedings of the 9th Biennial Engineering Mathematics and Applications Conference, EMAC-2009* (eds. Howlett, P., Nelson, M. & Roberts, A. J.) vol. 51 C360–C376 (2010).
18. Auxiliary Channel Three Hour Release.  
<https://www.gw-openscience.org/auxiliary/GW170814/>.
19. Damour, T. & Esposito-Farèse, G. Light deflection by gravitational waves from localized sources. *Phys. Rev. D* **58**, 044003 (1998).
20. Larchenkova, T. I., Lutovinov, A. A. & Lyskova, N. S. INFLUENCE OF THE GALACTIC GRAVITATIONAL FIELD ON THE POSITIONAL ACCURACY OF EXTRAGALACTIC SOURCES. *Astrophys. J.* **835**, 51 (2017).